Chemical Kinetic Interactions and Sensitivity Analyses for 2-Ethylhexyl Nitrate-doped PRF91 using a Reduced Mechanism

Seokwon Cho[a], Dario Lopez-Pintor[a*] and Scott Goldsborough[b]

[a] *Sandia National Laboratories, 7011 East Avenue, Livermore, CA 94550, USA*
[b] *Argonne National Laboratory, 9700 S. Cass Avenue, Lemont, IL 60439, USA*

Abstract

A numerical and experimental investigation about the chemical kinetic interactions between 2-ethylhexylnitrate (EHN) and PRF91 was performed in this study. Rapid compression machine experiments were conducted to investigate the effect of EHN on the autoignition reactivity of the fuel, and a reduced chemical kinetic mechanism was developed including an EHN sub-model. Experiments showed that the ignition delay decreases as the fuel is doped with EHN, but the effect of the doping level of EHN on the ignition is highly non-linear. Moreover, experiments showed that the EHN effectiveness is lowest during the transition between the low-temperature regime and the negative temperature coefficient (NTC) regime, and it rapidly increases as the temperature increases. Both detailed and (developed) reduced mechanisms were validated against the experimental results, allowing a more in-depth EHN-fuel chemistry study. Additionally, ignition delay sensitivity and EHN effectiveness sensitivity analyses were performed with the reduced mechanism to identify the reactions that control the interaction between EHN and the fuel. As the result, EHN thermal decomposition is only relevant for very low temperatures. The chemistry of EHN-doped fuel is more sensitive to intermediate temperature reactions than that of straight fuel, especially at lower temperatures, due to the effect of EHN on the NTC behavior of the fuel. Finally, the chemistry of EHN-doped fuel is very sensitive to NO_2-to-NO reactions, especially at high temperatures, because these reactions transform the NO_2 generated by EHN into NO, which is a very effective fuel reactivity enhancer.

Keywords

Rapid-compression machine; 2-ethylhexyl nitrate; Gasoline autoignition; Chemical kinetics; Detailed mechanism; Reduced mechanism

1. Introduction

Autoignition reactivity improvers (also known as cetane improvers), such as 2-ethylhexyl nitrate (EHN), have been used for years to enhance the autoignition quality of diesel fuel [1], increasing the flexibility of refinery processes and providing a mechanism for catalytic cracking products of heavy crude-oil distillates with low ignition quality to meet the legal requirements for market diesel [2]–[4]. Autoignition reactivity improvers have also been demonstrated to enhance the reactivity of gasoline, providing a promising pathway to tune the ignition quality for advanced compression ignition (ACI) engines that operate with low-temperature combustion modes, such as

* Corresponding author: Dario Lopez-Pintor, dlopezp@sandia.gov

Homogeneous Charge Compression Ignition (HCCI) engines [5]–[7] and Reactivity Controlled Compression Ignition (RCCI) engines [8]–[11].

More recently, the use of EHN-doped gasoline has enabled a new high-efficiency and low-emissions engine technology called Low-Temperature Gasoline Combustion (LTGC) with Additive-Mixing Fuel Injection (AMFI) [12], [13]. This combustion process is based on dosing a small, variable amount of EHN into the gasoline fuel on a cycle-by-cycle on-demand basis, which adjusts the fuel's reactivity for achieving fast and robust combustion control. LTGC-AMFI engines have demonstrated 10% to 25% higher efficiencies than a modern, equivalent-size, market-leading diesel engine, with two orders of magnitude lower engine-out NO_x and barely detectable soot emissions [12]. Moreover, studies have shown that the effectiveness of EHN for enhancing the fuel's autoignition reactivity increases with some high-renewable-content fuels compared to regular gasoline [14], providing a promising pathway to reduce the carbon footprint of internal combustion engines.

The decomposition of EHN has been extensively investigated [1], [15], [16]. It is widely accepted that thermal decomposition of EHN occurs via N-O cleavage, and chemical kinetics of EHN is traditionally described by a two-step reaction mechanism, by which EHN decomposes first to 2-ethylhexyloxy radical (EHO) and NO_2, and EHO decomposes to form other radicals, primarily 3-heptyl radical and formaldehyde [17], [18]. However, this simplified model has been unable to accurately reproduce experimental results from well-controlled facilities such as shock tubes [17], [19], rapid compression machines (RCMs) [18], [19], or research engines [20], which limits the investigation of the chemical interactions between EHN and other fuels.

A comprehensive mechanism for EHN decomposition was developed and validated in a recent investigation [21]. This mechanism expanded the two-step mechanism mentioned above by including alternative decomposition reactions of EHN, such as by radical attack, EHN ethanolysis, alternative EHO unimolecular decomposition reactions and EHO oxidation. The mechanism was integrated into a detailed mechanism for gasoline surrogates [22] and validated against shock

tube experiments of EHN-doped n-heptane and HCCI research engine experiments of EHN-doped gasoline. Additionally, the authors used a combined EHN-gasoline mechanism to understand the fundamentals of EHN chemistry and the mechanisms by which EHN affects the reactivity of a gasoline surrogate fuel. The authors concluded that, under ACI engine-like conditions, EHN decomposition generates NO_2 and a combination of 85%-mole of 3-heptyl radical and formaldehyde, plus 15% of 1-butyl radical and butoxy diradical. Moreover, it was concluded that 3-heptyl radical and 1-butyl radical are the most responsible for the effect of EHN on enhancing the reactivity of the fuel. These results are in agreement with those of other investigations, also concluding that 3-heptyl radical is the primary species responsible for the enhancing effect of EHN on the fuel's autoignition [17], [23], [24]. However, the reactions that control the EHN effectiveness were not identified in these studies.

There are several experimental investigations on the effects of EHN on diesel-like fuels under well-controlled conditions [1], [16], [17], [25]. However, there are only a few studies that experimentally investigated the chemistry fundamentals of the interactions between EHN and gasoline-like fuels in shock tubes or RCMs [18]. Moreover, the majority of these experimental studies were performed at stoichiometric conditions [18], whereas typical ACI engines operates with lean fuel-air mixtures.

In this paper, the chemical kinetic interactions between EHN and the gasoline surrogate PRF91 (primary reference fuel that consists of 91%$_{vol}$ iso-octane and 9%$_{vol}$ n-heptane) are studied experimentally in an RCM. Mixtures are tested at lean conditions to represent ACI engine operation. Furthermore, these experiments are used to further validate and improve the EHN mechanism proposed in [21]. Finally, sensitivity analyses are performed to identify the reactions to which the EHN effect is most sensitive.

2. Methodology

2.1. Experimental facility and parametric study

Experimental measurements are performed in Argonne National Laboratory (ANL)'s RCM facility. The facility consists of a twin opposed-piston, hydraulically-driven RCM. The RCM has been used in multiple previous investigations [18], [26]–[28], so the description of the RCM is covered briefly in this paper. The main specifications of the RCM are listed in Table 1. Creviced pistons were used to capture roll-up vortices created by the piston motion during the compression process, minimizing fluid-dynamic phenomena in the combustion chamber, ensuring a quasi-quiescent bulk gas and improving mixture homogeneity. The compression ratio of the RCM was kept constant at 14.3:1 during the study. The combustion chamber pressure was measured using a Kistler 601A piezoelectric pressure transducer that was mounted in the side of the combustion chamber wall, and the signal was amplified with a Kistler SCP-Slim amplifier. The configuration and settings used in this investigation are equivalent to those shown in [18].

Table 1. RCM specifications.

Bore	50.8	*mm*
Clearance height at end of compression	26.5	*mm*
Combustion chamber volume at end of compression	53.7	cm^3
Crevice volume	~9.1	cm^3
Compression time	19.6	*ms*
Geometric compression ratio	14.3:1	-
Effective compression ratio	10.2:1	-

The fuel used in this investigation was PRF91. Equivalence ratio was defined as the ratio of the actual fuel/air mass ratio to the stoichiometric fuel/air mass ratio, and tests were performed at an equivalence ratio of 0.72 and an oxygen mole fraction equal to 15%. Lean conditions were selected to closely represent the typical operating conditions of gasoline ACI engines. The fuel-air mixture was diluted either with pure nitrogen or with a mixture of 25% nitrogen + 75% argon, depending on the desired compression temperature. The dilution was required to allow measuring the ignition delay of EHN-doped fuel, which would, otherwise, be difficult to discern due to highly enhanced reactivity. Four different doping levels of EHN were tested: $0\%_{vol}$, $0.1\%_{vol}$, $1.0\%_{vol}$ and $3.0\%_{vol}$.

Test mixtures were prepared in an external vessel heated to 35°C. Gases were dosed based on their partial pressures and liquid fuel was delivered by a fuel injector. The fuel-gas mixture was kept in the tank for 120 min to ensure that the fuel was fully vaporized[1] and the mixture was homogeneous. The temperature of the combustion chamber was controlled by electrical heating elements. For each temperature setting, experiments were performed after a 30 min period for achieving thermal equilibrium. Similarly, each test sample was allowed to heat and homogenize for 7 min inside the combustion chamber to minimize thermal and mixture stratifications. The combustion chamber was vacuumed after each test to avoid test-to-test contamination.

Compression temperatures were swept from approximately 675 K to 1030 K by varying the initial temperature from 300 K to 373 K and by changing the composition of the dilution gas (pure nitrogen, or 25% nitrogen + 75% argon). The measured compression pressure was kept constant at 21 bar ± 1.0 bar for all the tests. The compression temperature was calculated based on the measured pressure signal and the composition of the mixture using an adiabatic core model [29]. At each condition, the test was conducted twice to ensure the experimental repeatability.

First-stage and second-stage (main) ignition delays were defined as the time from the end of compression to their associated maximum pressure rise rate. The end of compression was based on the time of peak pressure for a non-reactive undoped mixture, as explained in [18]. This approach is required for conditions where heat is released during the compression process, as happens in many of the conditions of this study. Note that, based on the previous definition of the ignition delay, negative ignition times are possible if the mixture autoignites before the end of compression. This is analogous to engine combustion phasings before top dead center.

2.2. Chemical kinetic simulations

ANSYS CHEMKIN-PRO is the software used for the chemical-kinetics simulations and analyses. A 0-D closed adiabatic homogeneous reactor was used to replicate the RCM experiments. The

[1] For 3.0%vol EHN experiments, the tank was heated to 50°C to ensure EHN vaporization.

adiabatic core hypothesis, that is widely used for RCM 0-D simulations [18], [30]–[33], was used in this work. The experimentally measured pressure signal under non-reacting conditions was used to characterize the wall heat losses of the RCM by defining a hypothetical volume profile. The volume profile represents the volume of an adiabatic gas core in the combustion chamber during the whole period including the compression process, and it was imposed as a time-varying boundary condition in the simulations along with the experimental temperature and pressure at the start of compression. This way, the simulations incorporated the chemical reactions that may occur during the compression process. Also, the experimental uncertainties was primarily caused by piston trajectory measurement error [18] so a correction was made by moderately adjusting the initial temperature and pressure of the simulations to achieve numerical compressed thermodynamic conditions consistent with those of the experiments. Iterations were made to keep the error in temperature after the compression within ± 5 K with the experimental result.

Two different chemical kinetic mechanisms were used during the simulations in this study. First, the Lawrence Livermore National Laboratory (LLNL) Co-Optima 2020 detailed mechanism for gasoline surrogates [22], which consists of 4164 species and 18636 reactions, was chosen and it is, to the best of our knowledge, one of the most state-of-the-art mechanisms for gasoline-like fuels available. Second, a reduced mechanism for PRF mixtures was developed by Sandia National Laboratories (SNL) to allow reasonably reduced computational cost for chemical sensitivity analyses. This PRF mechanism was generated by reducing the LLNL Co-Optima 2020 mechanism based on a large set of ignition delay times of PRF0, 25, 50, 75 and 100. Ignition delays were obtained from closed adiabatic homogeneous constant-volume reactor simulations with variations in pressure from 30 to 75 bar, in oxygen content of 15% and 21%, in equivalence ratio from 0.3 to 5.0 and in temperature from 530 K to 1100 K, respectively. For reduction of the detailed mechanism, Direct Relation Graph (DRG) [34] method was applied, targeting the fuel's ignition delay with a relative tolerance of 15%. The following species were included in the initial set of species of the DRG method: n-heptane and iso-octane (fuels), O_2, N_2, CO_2 and H_2O (main

159 reactants and products), NO and NO_2 (for NO_x chemistry), C_2H_2 (soot precursor) and OH in both
160 excited and ground states (for combustion diagnosis). During the method, the chemistry of ethanol
161 and EHN ethanolysis [21] were not considered. The mechanism obtained from this procedure
162 consists of 1163 species and 6415 reactions. This mechanism was further reduced to 753 species
163 and 4223 reactions by using the Direct Relation Graph with Error Propagation (DRGEP) method
164 [35] with the same target and initial set of species described above. Finally, the DRGEP +
165 sensitivity analysis + optimization method was applied [36]. Sensitivity analyses were performed
166 to identify the reactions to be optimized, with a maximum number of optimized reactions equals
167 to 30 (i.e., 30 the most sensitive reactions to ignition delay were optimized) and allowing
168 adjustments of only pre-exponential coefficients of each Arrhenius expression which defines the
169 specific reaction rate. As the result of this step, the final version PRF mechanism is composed by
170 248 species and 1428 reactions. The PRF mechanism was evaluated by comparing against the
171 well-validated detailed mechanism from LLNL, and results are shown in Appendix A. Moreover,
172 the PRF mechanism was further validated against the RCM experiments of this study, as will be
173 shown in the following section.
174 The EHN sub-mechanism proposed by Lopez-Pintor and Dec [21] was used in this investigation.
175 This sub-mechanism consists of 38 species and 33 reactions, including reactions regarding EHN
176 thermal unimolecular decomposition, EHN decomposition by radical attack and EHN ethanolysis.
177 In this study, the sub-mechanism was integrated into the LLNL Co-Optima 2020 mechanism as
178 explained in [21]. For the integration of the EHN sub-mechanism into the reduced PRF
179 mechanism, EHN ethanolysis reactions were discarded due to the absence of ethanol chemistry
180 in the PRF mechanism. This simplification is highly unlikely to affect the simulation accuracy of
181 EHN-doped PRFs.
182 To understand the impact of doping EHN to fuel, EHN effectiveness is defined as the ratio
183 between the main ignition delay of straight fuel and EHN-doped fuel, as the follow:

$$EHN\ effectiveness\ (\eta) = \frac{\tau_{no\ EHN}}{\tau_{EHN}} \quad (1)$$

where τ is ignition delay.

Sensitivity analyses were performed at four different temperatures: 600 K, 725 K, 850 K and 975 K, which represent the low-temperature, cold-side of NTC, hot-end of NTC and high-temperature autoignition regimes, respectively; and at four EHN doping levels: 0%$_{vol}$, 0.1%$_{vol}$, 1.0%$_{vol}$ and 3.0%$_{vol}$; for PRF91 at equivalence ratio 0.72 and 15% O_2, which aligned with the conditions of the RCM experiments. Simulations were carried out in 0-D closed adiabatic constant-volume reactors. Here, two different sensitivity analyses were performed. First, the sensitivity coefficients for the ignition delay were calculated at the time of ignition as follows:

$$S_i = -\frac{A_i}{\tau}\frac{\partial \tau}{\partial A_i} \propto \frac{A_i}{T_0}\frac{\partial T}{\partial A_i}\bigg|_{t=\tau} \quad (2)$$

where S_i is the ignition delay sensitivity coefficient of reaction i, T is temperature, while A_i represents the pre-exponential factor. The minus sign in equation 2 is used so that the positive S_i values means reaction i increases the autoignition reactivity of the fuel (i.e., shortens the ignition delay). This definition may or may not be conventional, but was applied by considering negative correlation between changes in temperature and ignition delay. The partial derivative of temperature in the equation corresponds to the temperature sensitivity to the pre-exponential factor A_i. Given that the temperature rise is uniquely caused by the ignition event, A_i is believed to be proportional to ignition delay sensitivity at the time of ignition. Sensitivity coefficients were normalized by the initial temperature of the simulation (T_0) to avoid any bias due to different initial conditions.

Second, sensitivity coefficients for the EHN effectiveness (enhancement effect) on fuel's reactivity were calculated as follows:

$$R_i = \frac{A_i}{\eta}\frac{\partial \eta}{\partial A_i} = \frac{A_i}{\tau_{no\ EHN}}\frac{\partial \tau_{no\ EHN}}{\partial A_i} - \frac{A_i}{\tau_{EHN}}\frac{\partial \tau_{EHN}}{\partial A_i} = S_{i,EHN} - S_{i,no\ EHN} \quad (3)$$

where R_i is the EHN sensitivity coefficient of reaction i, η is the EHN effectiveness and S_i is the ignition delay sensitivity coefficient of reaction i as defined by equation 2.

3. Results

3.1. RCM experiments and simulations

Experiments with straight PRF91 (with no EHN) were used to evaluate the accuracy of the two mechanisms described previously. Figure 1 shows logarithmic-scaled first-stage ignition delay (a) and main ignition delay (b) from the RCM experiment (solid line), simulation with the detailed mechanism (dashed line) and simulation with the reduced mechanism (dotted line). Simulations over-estimate the first-stage ignition delay for the hot-end of the NTC zone (T > 780 K). However, the overall trends are decently replicated by the simulations and both the detailed and the reduced mechanisms show consistent results.

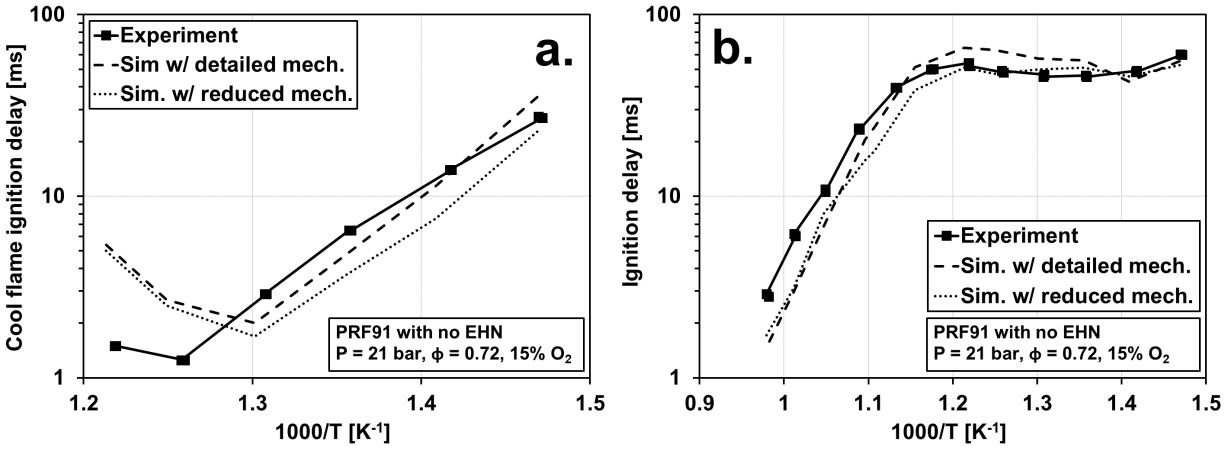

Figure 1. First-stage ignition delay (a) and main ignition delay (b) vs. inverse compressed temperature for experiment (solid line), simulation using detailed mechanism (dashed line), and simulation using reduced mechanism (dotted line).

Figure 2 plots the experimental first-stage ignition delay (a) and main ignition delay (b) for four different doping levels of EHN from 0%$_{vol}$ to 3.0%$_{vol}$. The log-modulus transformation ($y = sign(\tau) \cdot log(1 + |\tau|)$) is used to plot negative ignition delay values in logarithmic scale. The experiment shows that the ignition delay decreases as the fuel-EHN doping level increases. The NTC zone of the fuel shifts to lower temperatures as the fuel doping level increases. However, the effect of the doping level of EHN on the ignition is highly non-linear. Both ignition delays rapidly

decrease when the EHN doping level increases from 0%$_{vol}$ (straight fuel) to 0.1%$_{vol}$, whereas the reactivity enhancement becomes insignificant for higher EHN doping values. This suggest that the EHN effect on fuel's reactivity is saturated at a certain EHN doping level. This result agrees with those of previous investigations in RCMs and ACI engines [9], [12], [18], [37].

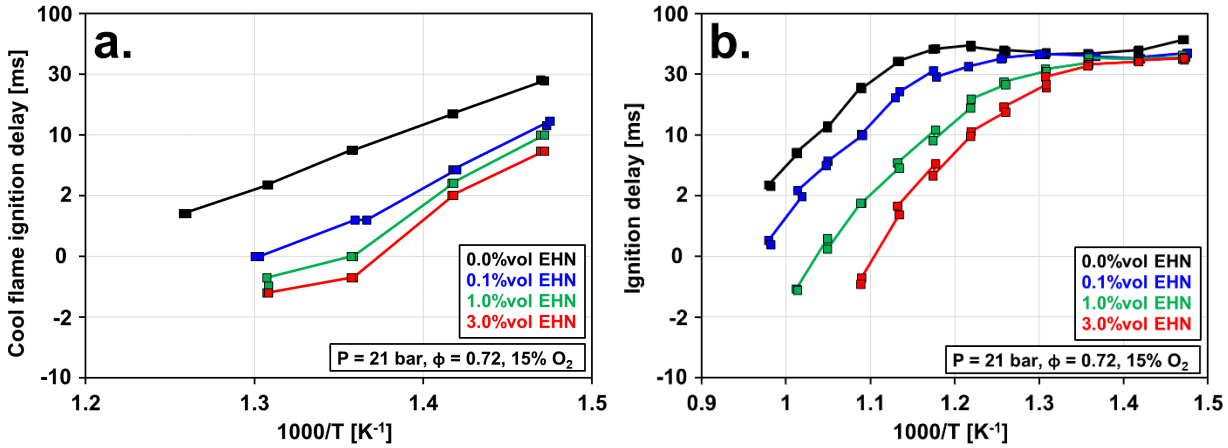

Figure 2. First-stage ignition delay (a) and main ignition delay (b) vs. compression temperature for the RCM experiments using four different EHN doping levels: 0%$_{vol}$ (black), 0.1%$_{vol}$ (blue), 1.0%$_{vol}$ (green) and 3.0%$_{vol}$ (red).

Figures 3 and 4 show the first-stage ignition delay and the main ignition delay, respectively, for the data shown in Figure 2. Results of the RCM experiment and the corresponding numerical simulation are presented. Although plots for both mechanisms in Figure 3 show slight discrepancies at high temperature regime (800 K to 950 K) in first-stage ignition delay, but both the detailed and the reduced mechanisms show reasonably good accuracy in reproducing the experimental trends in first-stage ignition delay. The simulation results with both mechanisms showed excellent behavior for predicting the main ignition delay as shown in Figure 4. Importantly, the reduced mechanism exhibits a remarkable performance to follow the detailed mechanism in all cases.

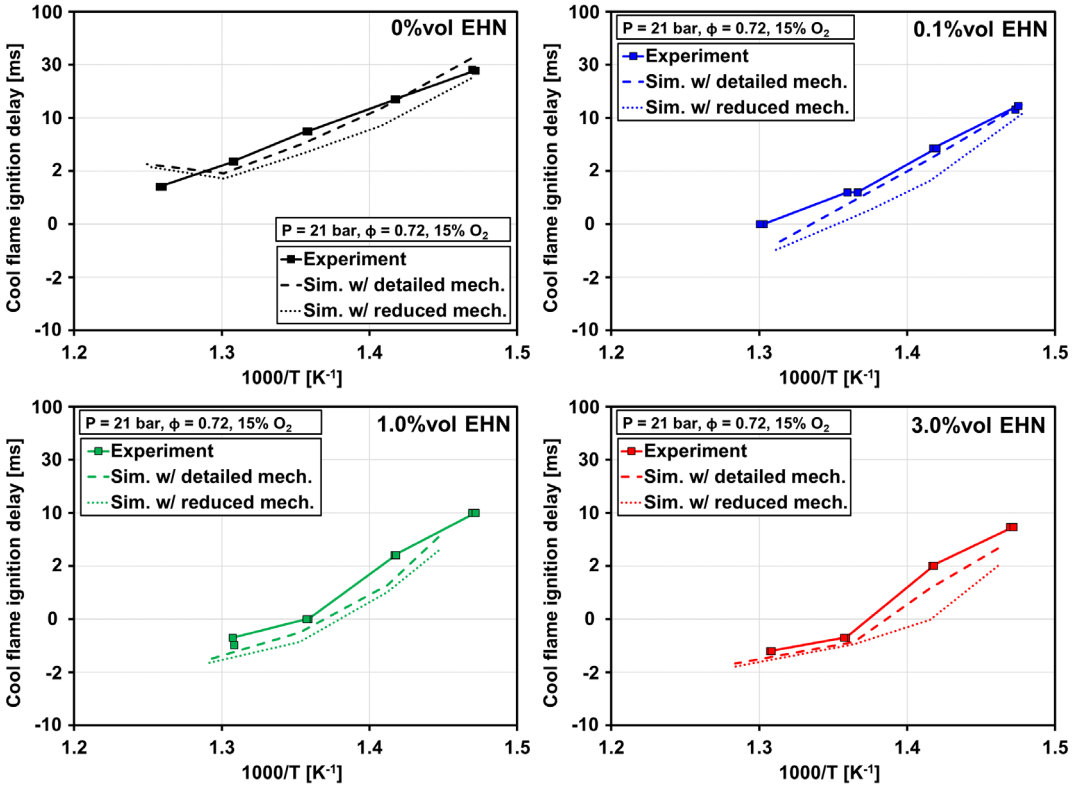

Figure 3. First-stage ignition delay vs. compression temperature for experiment and simulations using four EHN doping levels: 0%$_{vol}$ (black), 0.1%$_{vol}$ (blue), 1.0%$_{vol}$ (green) and 3.0%$_{vol}$ (red).

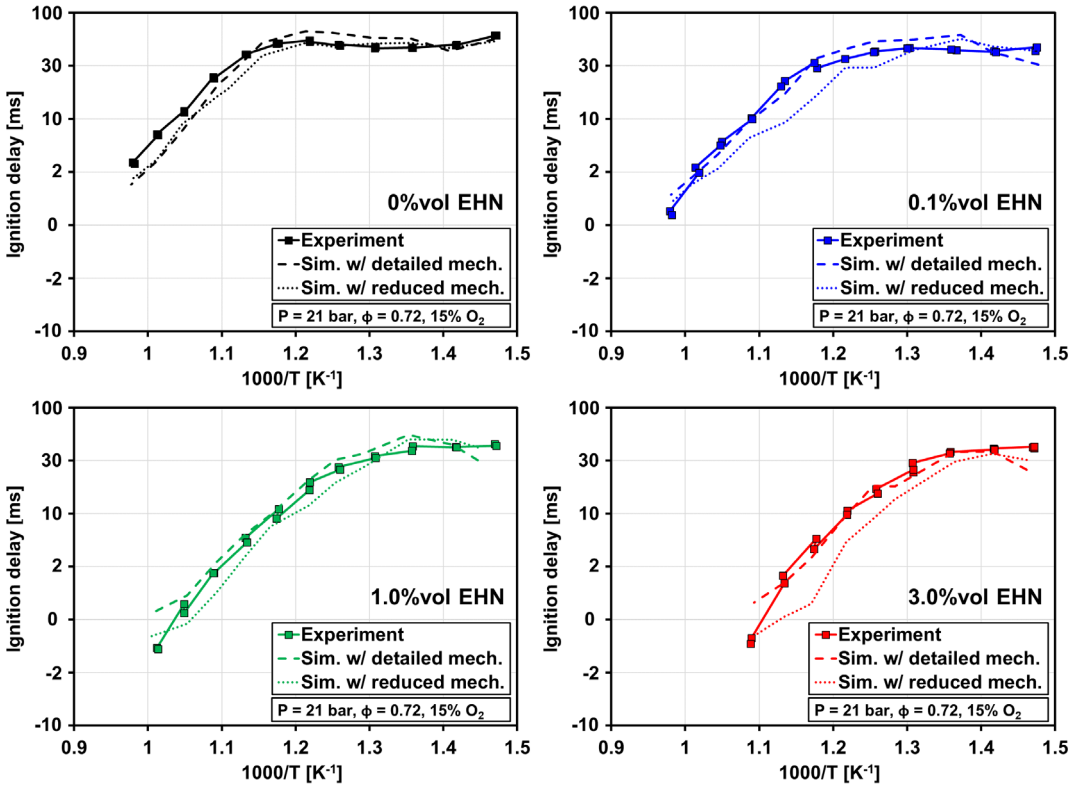

Figure 4. Main ignition delay vs. compression temperature for experiment and simulations using four EHN doping levels: 0%$_{vol}$ (black), 0.1%$_{vol}$ (blue), 1.0%$_{vol}$ (green) and 3.0%$_{vol}$ (red).

Figure 5 shows the EHN effectiveness at different doping level of EHN in the experiments and simulations. Negative and close-to-zero ignition delay times were obtained during this investigation due to the remarkable enhancement of fuel reactivity by EHN, so the calculated effectiveness could be misleading and counterintuitive when the ignition delays are not referenced to earlier timings. Therefore, the ignition delay values for the calculation of the results shown in Figure 5 are referenced to the start of the compression process instead of to the end of compression. The higher the EHN effectiveness, the higher the impact of EHN on the fuel's ignition delay, so EHN effectiveness values close to 1 mean that EHN has less advantage on the reactivity enhancement. As indicated earlier, a non-linearity of the effect was found: the increase in EHN effectiveness when increasing EHN dosage from 1.0%vol to 3.0%vol is not as high as when the EHN dosage is increased from 0.1%vol to 1.0%vol. This suggests that the effect of EHN may saturate at a given dosing level, so that autoignition reactivity of the fuel does not benefit from higher EHN concentrations than a certain threshold EHN level.

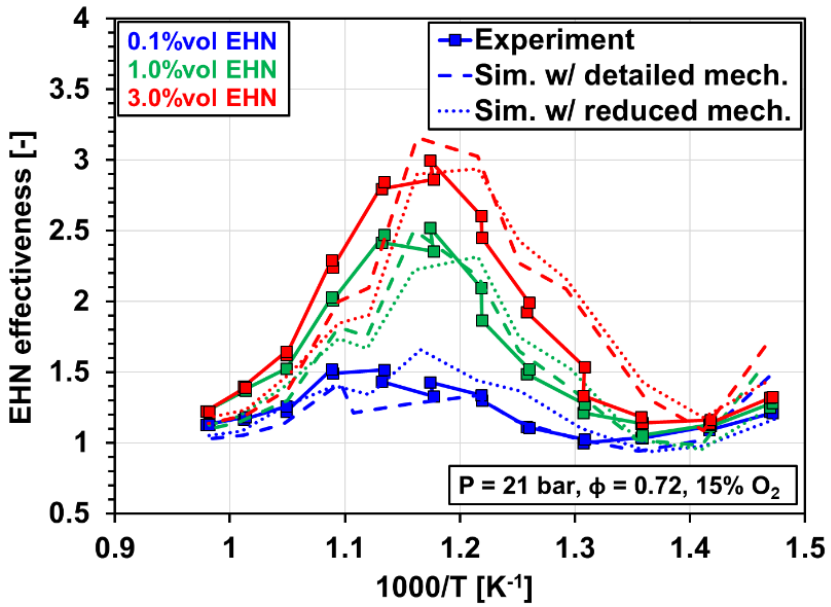

Figure 5. EHN effectiveness for experiments and simulations using different EHN doping levels.

The greatest limitation in the EHN effect is observed at the transition between the low-temperature regime and the NTC regime. The EHN effectiveness rapidly increases (i.e., the EHN effect on

reactivity becomes more pronounced) as the temperature increases, up to the maximum value in NTC regime temperature. This is because EHN shifts the NTC zone of the fuel to lower temperatures as previously discussed (see Figure 2). Therefore, the transition from NTC to the high-temperature regime occurs at lower temperatures for EHN-doped fuel compared to the straight fuel, leading to a more pronounced EHN effect. The EHN effectiveness decreases in the high-temperature regime, which is in good agreement with the numerical results shown in [21]. This is because EHN primarily acts on the low-temperature chemistry of the fuel, so the effect at high temperatures (above 1000 K) is marginal. Unfortunately, there is no sophisticated experimental investigation on the EHN effectiveness during the low-temperature regime (temperature lower than 650 K). However, results presented in [21] suggest that the EHN mechanism accurately reproduces the low-temperature chemistry of EHN-doped n-heptane as measured in a shock tube, giving confidence on the ability of the mechanism to perform analyses at conditions in the low-temperature regime. According to the results presented in [21], EHN is very effective in enhancing reactivity at low temperatures because OH radicals are generated at early phase during ignition process, accelerating the low-temperature chemistry.

3.2. Sensitivity analyses

Sensitivity analyses were conducted by identifying the reactions that are most sensitive to the EHN doping and alters ignition delay significantly. For the analyses, sensitivity coefficients described in equations 2 (S_i) and 3 (R_i) for all the reactions included in the reduced mechanism were obtained. The reactions are classified according to their reaction class and the results are discussed in this section. Sensitivity analyses with the detailed mechanism were not performed due to substantial computational cost.

3.2.1. Sensitivity to ignition delay

Figure 6 shows the normalized sensitivity coefficients of ignition delay for straight PRF91 (left) and for PRF91 doped with 1.0%$_{vol}$ of EHN (right) at four different temperatures that represent

different ignition regimes: 600 K (low-temperature regime), 725 K (cold-side of NTC regime), 850 K (hot-end of NTC regime) and 975 K (high-temperature regime). In the figure, reactions are sorted according to their reaction class. Dehydrogenation of iso-octane and n-heptane by OH attack are considered separately from other hydrogen abstraction reactions to better evaluate the impact of EHN on fuel-OH reactions, because EHN forms OH radicals when it decomposes. A positive sensitivity coefficient value indicates that that the reaction tends to increase the reactivity of the fuel (i.e., decrease the ignition delay) and vice versa. For better clarity, the temperature regimes shown in Figure 6 are discussed separately. At a given temperature regime, the results of the sensitivity analyses are first discussed for straight fuel. For EHN-doped fuel, only the differences compared to the straight fuel are discussed. It should be mentioned that similar results were obtained regardless of the EHN doping level.

Low-temperature regime (600 K)

- Straight fuel:

For the low-temperature regime, the ignition delay is very sensitive to fuel dehydrogenation by OH attack, which is the key initiation reaction for fuel decomposition. The increased rate of production (ROP) of IC8-5R radical decreases the ignition delay (positive sensitivity coefficient), whereas the higher ROP of IC8-4R increases the ignition delay (negative sensitivity coefficient). This is because IC8-5R generates ketones + OH radicals that promote the low-temperature chain branching mechanism (see the first two reactions of the OH formation group). On the other hand, IC8-4R leads to long, branched and stable olefins that tend to reduce the reactivity, eventually causing the NTC behavior of the fuel.

The ignition delay also shows high sensitivity to isomerization reactions that involve the formation of ROOH radicals from ROO species and to O_2 addition reactions that involve the formation of OOROOH species from ROOH radicals. Both isomerization and O_2 addition reactions have positive ignition delay sensitivity coefficients, which means that the low-temperature chain

branching mechanism accelerates if these reactions are enhanced. Interestingly, HO_2 elimination shows a high negative sensitivity coefficient because ROO radicals formed from IC8-4R lead, via HO_2 elimination, to long, branched and stable olefins, which tend to decrease the overall reactivity of the mixture. Finally, the ignition delay is also sensitive to the reactions that contribute to formation of OH radicals, which act as chain carriers and promote the fuel decomposition via the low-temperature chain branching mechanism.

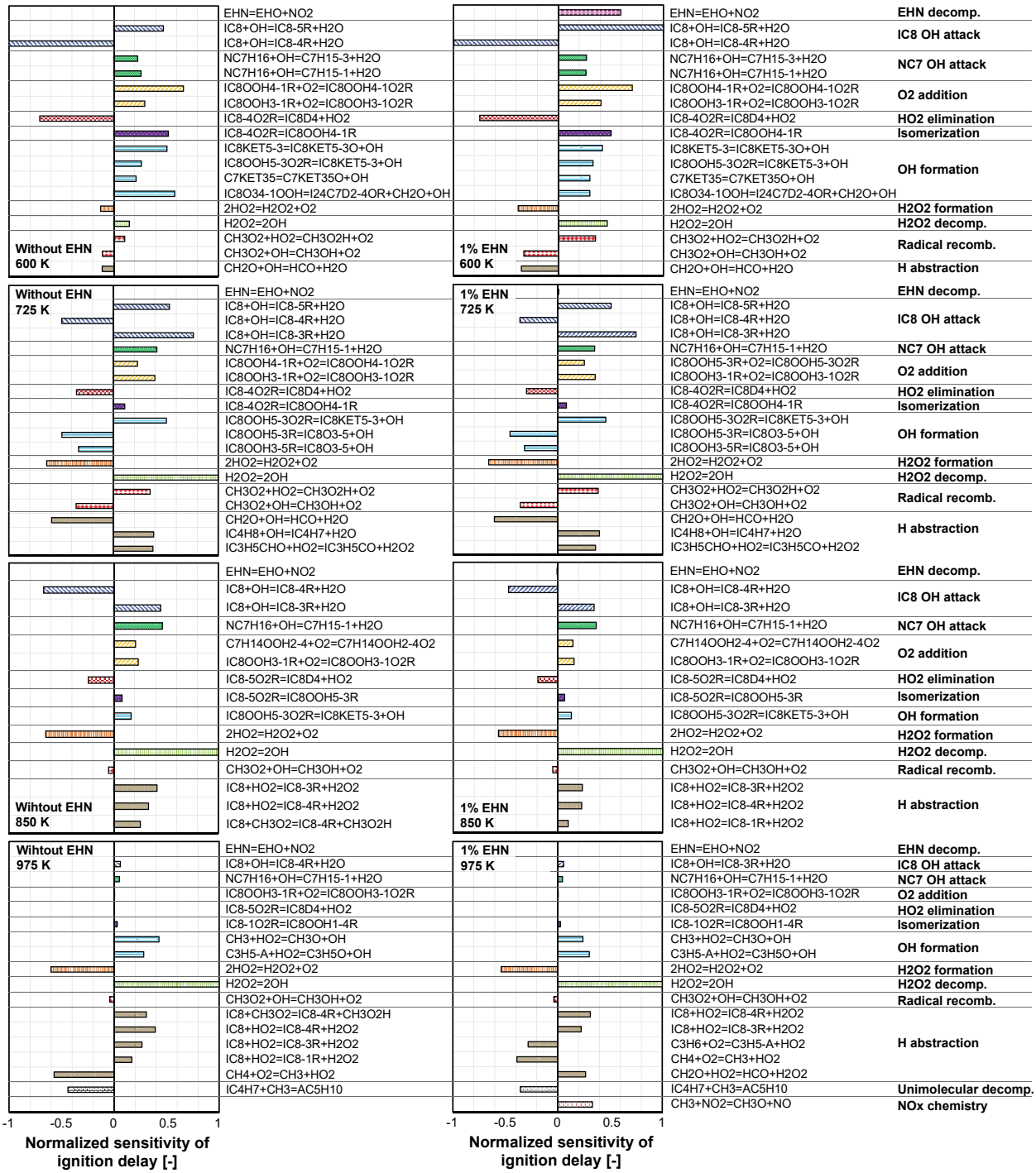

Figure 6. Sensitivity coefficients of ignition delay for straight PRF91 (left) and for PRF91 doped with 1.0%$_{vol}$ of EHN (right) at different temperatures. Reactions are sorted according to their reaction class.

- EHN-doped fuel:

The most notable thing is that the reactions related to EHN thermal decomposition have high and positive sensitivity coefficients at these low temperatures. It was shown that the higher the EHN doping level, the more sensitive the ignition delay was to this reaction. The ignition delay of EHN-doped fuel is less sensitive to OH formation reactions than straight fuel because EHN generates OH when it decomposes and, therefore, the autoignition process of EHN-doped fuel is less dependent of the OH radicals generated via the low-temperature chain branching mechanism of the fuel. Fuel dehydrogenation by OH attack are the most relevant reactions at this condition, since EHN acts on the fuel via OH chemistry.

Reactions that are important at the cold-side of the NTC regime (725 K) such as H_2O_2 formation, H_2O_2 decomposition and radical recombination are not as significant for the straight fuel at low temperature regime, where as those become important when the fuel is doped because EHN shifts the NTC zone to lower temperatures, as shown experimentally in Figures 2-4.

Cold-side of NTC regime (725 K)

- Straight fuel:

At the cold-side of the NTC regime, the ignition delay becomes less sensitive to the reactions that control the low-temperature chain branching mechanism: fuel dehydrogenation by OH, O_2 addition, isomerization, and HO_2 elimination reactions. Among all these reaction classes, the most distinctive change in the ignition delay is the significantly low sensitivity to ROO isomerization, and this is attributable to fast isomerization that does not cause a bottleneck for the ignition process at this temperature. Interestingly, two OH formation reactions that consist of the generation of OH and cyclo-ethers from ROOH radicals, exhibit large negative sensitivity coefficients becasue these cyclo-ethers are very stable and tend to decrease the reactivity of the mixture. H_2O_2 formation and, especially, H_2O_2 decomposition become the most impactful reactions during the NTC regime. When H_2O_2 decomposes, each mole of H_2O_2 generates two moles of OH that rapidly oxidize the intermediate hydrocarbon species to CO and trigger the main

ignition. Radical recombination and H abstraction reactions, which involve short-chain, partially-oxidized hydrocarbons formed during the intermediate-temperature stage of the ignition, also become more relevant at this condition.

- EHN-doped fuel:

Although EHN is added, the ignition delay is not sensitive to EHN thermal decomposition for temperatures higher than or equal to 725 K unlike in low-temperature regime. The decomposition is very fast for temperatures above 700 K range and, therefore, the reaction is not a bottleneck for the ignition process in this condition.

Hot-end of NTC regime (850 K)

For the hot-end of the NTC regime, the ignition delay becomes less sensitive to the reactions related to the low-temperature chain branching mechanism. As explained before, H_2O_2 chemistry controls the ignition during the NTC regime. Interestingly, fuel dehydrogenation reactions that involve HO_2 are almost as relevant as those that involve OH, presumably because HO_2 formation is promoted at these temperatures.

High-temperature regime (975 K)

- Straight fuel:

During the high-temperature regime, the ignition delay is no longer sensitive to low-temperature reactions. Notably, the ignition delay becomes sensitive to OH formation reactions that involve short, partially-oxidized hydrocarbons. The ignition delay is also sensitive to fuel dehydrogenation reactions that involve HO_2 and CH_3O_2 radicals, whereas H_2O_2 formation and decomposition are the two most important reactions for the ignition delay. Finally, the ignition delay becomes sensitive to unimolecular decomposition reactions that require high temperatures to occur.

- EHN-doped fuel:

The ignition delay of EHN-doped fuel is very sensitive to the NO_x chemistry, conversion of NO_2 to NO at this condition. Results for other EHN concentrations show that the higher the EHN doping

level, the more sensitive the ignition delay is to this reaction. Thermal decomposition of EHN generates NO_2, but has a marginal effect on the fuel's ignition delay. However, the ignition delay is very sensitive to the reaction $CH_3 + NO_2 = CH_3O + NO$ because it transforms the NO_2 generated by EHN into NO, and NO is a well-known reactivity enhancer as it generates OH radicals early in the ignition process.

3.2.2. Sensitivity to EHN effectiveness

This section presents the analysis on EHN effectiveness sensitivity that identifies which reactions the EHN effectiveness is more sensitive to. It should be noted that a reaction to which the ignition delay is not sensitive may still be highly relevant for the EHN effectiveness. Thus, reactions that were not identified in the previous analysis but can be important for EHN chemistry will be identified in this section.

Figure 7 shows normalized sensitivity coefficients of EHN effectiveness, as defined by equation 3, for PRF91 doped with 1.0%$_{vol}$ EHN at four different temperatures. Similar to Figure 6, the reactions are sorted by the class. A positive sensitivity coefficient means that the reaction tends to increase the EHN effectiveness, increasing the impact of EHN on the fuel's ignition delay, and vice versa.

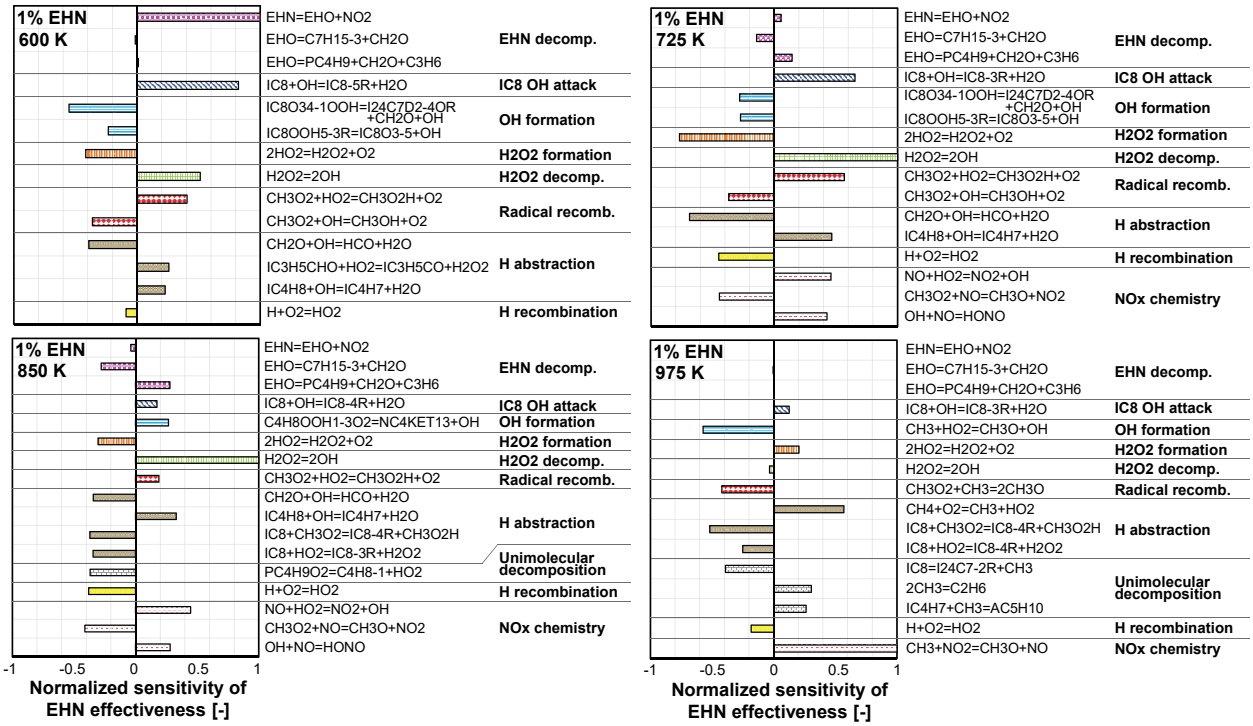

Figure 7. Sensitivity coefficients of EHN effectiveness for PRF91 doped with 1.0%$_{vol}$ of EHN at different temperatures. Reactions are sorted according to their reaction class.

<u>*Low temperature regime (600 K)*</u>

For the low-temperature regime, the EHN effectiveness is mainly controlled by EHN thermal decomposition, which is the bottleneck for EHN chemistry at this temperature. The EHN effectiveness is very positive-sensitive to fuel dehydrogenation by OH attack because EHN enhances the reactivity of the fuel primarily by generating OH radicals at early ignition process. OH formation reactions from the low-temperature chain branching mechanism show negative sensitivity coefficients and, therefore, are detrimental to the EHN effect. Reactions that are important at intermediate temperatures, such as H_2O_2 formation/decomposition, radical recombination and H abstraction of short intermediate hydrocarbons, are also relevant for the EHN effectiveness at low temperatures because adding EHN shifts the NTC zone of the fuel to lower temperatures.

<u>*Cold-side of NTC regime (725 K)*</u>

At the cold-side of the NTC regime, the EHN effectiveness is not sensitive to the EHN thermal decomposition reaction because the ambient temperature is high enough to rapidly decompose the EHN. Intermediate temperature reactions become very relevant and are the main controllers for the effectiveness at this condition. Interestingly, the EHN effectiveness becomes sensitive to the collisional recombination of atomic hydrogen via $H + O_2 = HO_2$, and shows a negative sensitivity coefficient. This recombination reaction acts as a sink of H radicals so tends to decrease the reactivity, and it tends to decrease the reactivity more for EHN-doped fuel than for straight fuel, decreasing the EHN effectiveness. This behavior is thought to be caused by the radicals generated by EHN, which accelerate the transition to intermediate-temperature chemistry where H recombination, HO_2 chemistry and H_2O_2 chemistry dominates. The ignition delay is not very sensitive to the H recombination reaction.

The figure shows high sensitivity to NO_x chemistry at this condition. As explained above, the thermal decomposition of EHN generates NO_2, which marginally affect the reactivity. However, there are several generative reactions for other NO_x species such as NO that significantly affect the reactivity leading to the high sensitivity of the EHN effectiveness.

Hot-end of NTC regime (850 K)

Under the hot-end of the NTC regime, the EHN effectiveness becomes less sensitive to intermediate temperature chemistry. However, H_2O_2 decomposition is still the most impactful reaction. The effectiveness is shown being sensitive to ethylhexyloxy radical (EHO) decomposition at this condition. This is because EHO generates either 3-heptyl radicals (that eventually form OH radicals through the n-heptane low-temperature chain branching reactions) or butyl radicals (that eventually form OH and CH_3 radicals), and butyl radical is a more effective reactivity enhancer than 3-heptyl radical. Therefore, the reaction associated with EHO to butyl radical shows a positive sensitivity coefficient and tends to increase the EHN effectiveness, whereas the radical reaction of EHO to 3-heptyl shows a negative value and decrease the

effectiveness. Collisional recombination of atomic hydrogen and NO_x chemistry are also relevant reactions for the effectiveness at this condition, as previously discussed for the cold-side of the NTC regime.

High-temperature regime (975 K)

For the high-temperature regime, the EHN effectiveness is most sensitive to NO_x chemistry, more specifically, to NO formation from NO_2 via CH_3. This reaction shows the greatest positive sensitivity coefficient and, therefore, increase the EHN effectiveness. It is attributed to transformation of NO_2, which is generated by EHN but not an effective ignition improver, to a very well-known strong ignition enhancer, NO [38]. Thus, if NO_2-to-NO reactions are promoted, the effect of EHN on fuel's reactivity is enhanced and the EHN effectiveness increase. Because the unimolecular decomposition reactions involve CH_3, the EHN effectiveness become dependent to such reactions at this condition.

4. Conclusions

A numerical and experimental investigation about the chemical kinetic interactions between EHN and PRF91 was performed in this study. Experiments carried out in the ANL RCM were used to investigate the effect of EHN on the autoignition reactivity of the fuel and to validate two chemical kinetic mechanisms, a detailed mechanism from LLNL and a SNL-developed reduced mechanism, which were combined with an EHN sub-model to allow EHN-fuel chemistry studies. Finally, to better understand the chemistry of EHN-doped fuel and to identify the impactful reactions for controlling the interaction between EHN and the fuel, sensitivities to ignition delay and EHN effectiveness were analyzed with the reduced mechanism. The summary of this work is the following conclusions:

- RCM experiments show that the ignition delay decreases as more EHN is doped to the base fuel (PRF91). However, the effect of the doping level of EHN on the ignition is highly

non-linear, suggesting that the EHN effect on fuel's reactivity might be saturated at a certain doping level.

- The LLNL detailed mechanism shows an excellent agreement with the RCM experiments for straight PRF91, and remarkable matching results are also obtained with SNL reduced mechanism. The combination of these mechanisms with the EHN sub-model also shows a reasonably good agreement with the experiments with EHN-doped fuel, properly capturing the EHN enhancing effect on the autoignition reactivity of the fuel across a range of temperature and doping levels. It is expected that developed reduced mechanism will play a significant role in reducing computational cost while holding a good accuracy for multi-dimensional simulations.
- RCM experiments show that the lowest EHN effectiveness locates near the temperature at which the condition transitions from low-temperature to NTC regime. The effectiveness rapidly increases as the temperature increases before the hot-end of NTC regime. This behavior comes from that EHN shifts the NTC zone to lower temperatures. Finally, the EHN effectiveness decreases again when temperature increases to the hot-temperature regime, because EHN has limited effect on intermediate- and high-temperature chemistry of the fuel.
- Sensitivity analyses show that the ignition delay is overwhelmingly sensitive to EHN thermal decomposition at low temperatures. Particularly at low temperatures, the ignition delay of EHN-doped fuel is more sensitive to intermediate temperature chemistry than that of straight fuel, because EHN shifts the NTC zone to lower temperatures. The ignition delay of EHN-doped fuel showed less dependency to fuel-generated OH radicals, due to the OH generation from EHN decomposition. The ignition delay of EHN-doped fuel is shown to be very sensitive to NO_2-to-NO reactions at high-temperature conditions by presence of NO which significantly enhances the ignition whereas NO_2 barely affects.

Acknowledgements

Michael V. Johnson and Colin Banyon are thanked for assisting with measurements in the Rapid Compression Machine Facility in Argonne National Laboratory. Namho Kim is thanked for insightful review of this paper. This study was performed at the Combustion Research Facility, Sandia National Laboratories, Livermore, CA, and was supported by U.S. Department of Energy, Office of Vehicle Technologies.

Sandia National Laboratories is a multi-mission laboratory managed and operated by National Technology and Engineering Solutions of Sandia, LLC., a wholly owned subsidiary of Honeywell International, Inc., for the U.S. Department of Energy's National Nuclear Security Administration under contract DE-NA0003525. The work at ANL was conducted under the auspices of the U.S. Department of Energy, Contract No. DE-AC02-06CH11357. The views expressed in the article do not necessarily represent the views of the U.S. Department of Energy or the United States Government.

Definitions/Abbreviations

ACI	Advanced Compression Ignition
AMFI	Additive-Mixing Fuel Injection
ANL	Argonne National Laboratory
DRG	Directed Relation Graph
DRGEP	Directed Relation Graph with Error Propagation
EHN	2-ethylhexylnitrate
EHO	2-ethylhexyloxy radical
HCCI	Homogeneous charge compression ignition
LLNL	Lawrence Livermore National Laboratory
LTGC	Low temperature gasoline compression-ignition
NTC	Negative temperature coefficient
PRF	Primary reference fuels
RCCI	Reactivity Controlled Compression Ignition
RCM	Rapid compression machine
ROP	Rate of production
SNL	Sandia National Laboratories
A_i	Pre-exponential factor of the specific reaction rate of reaction i
R_i	Sensitivity coefficient of EHN effectiveness of reaction i
S_i	Ignition delay sensitivity coefficient of reaction i
ϕ	Equivalence ratio
P	Pressure
T	Temperature
η	Effectiveness
τ	Ignition delay

References

[1] T.-M. Li and R. F. Simmons, "Twenty First Symposium (International) on Combustion," *The Combustion Institute,* vol. Pittsburgh, pp. 455–462, 1988.

[2] S. Sarıkoç, *Fuels of the Diesel-Gasoline Engines and Their Properties*. IntechOpen, 2020.

[3] T. Mammadova *et al.*, “Production of diesel fractions by catalytic cracking of vacuum gas oil and its mixture with cottonseed oil under the influence of a magnetic field,” *Egyptian Journal of Petroleum*, vol. 27, no. 4, pp. 1029–1033, Dec. 2018, 10.1016/j.ejpe.2018.03.010.
[4] P. Ghosh, “Predicting the Effect of Cetane Improvers on Diesel Fuels,” *Energy Fuels*, vol. 22, no. 2, pp. 1073–1079, Mar. 2008, https://doi.org/10.1021/ef0701079.
[5] C. Ji, J. E. Dec, J. Dernotte, and W. Cannella, “Effect of Ignition Improvers on the Combustion Performance of Regular-Grade E10 Gasoline in an HCCI Engine,” *SAE Int. J. Engines*, vol. 7, no. 2, pp. 790–806, Apr. 2014, https://doi.org/10.4271/2014-01-1282.
[6] C. Ji, J. Dec, J. Dernotte, and W. Cannella, “Boosted Premixed-LTGC / HCCI Combustion of EHN-doped Gasoline for Engine Speeds Up to 2400 rpm,” *SAE Int. J. Engines*, vol. 9, no. 4, Oct. 2016, doi:10.4271/2016-01-2295.
[7] V. Hosseini, W. S. Neill, H. Guo, W. L. Chippior, C. Fairbridge, and K. Mitchell, “Effects of different cetane number enhancement strategies on HCCI combustion and emissions,” *International Journal of Engine Research*, vol. 12, no. 2, pp. 89–108, 2011, https://doi.org/10.1177/1468087410395873.
[8] R. Hanson, S. Kokjohn, D. Splitter, and R. D. Reitz, “Fuel Effects on Reactivity Controlled Compression Ignition (RCCI) Combustion at Low Load,” *SAE Int. J. Engines*, vol. 4, no. 1, pp. 394–411, Apr. 2011, https://doi.org/10.4271/2011-01-0361.
[9] J. Kaddatz, M. Andrie, R. D. Reitz, and S. Kokjohn, “Light-Duty Reactivity Controlled Compression Ignition Combustion Using a Cetane Improver,” *SAE Technical Paper 2012-01-1110*, Apr. 2012, https://doi.org/10.4271/2012-01-1110.
[10] A. B. Dempsey, N. R. Walker, and R. D. Reitz, “Effect of Cetane Improvers on Gasoline, Ethanol, and Methanol Reactivity and the Implications for RCCI Combustion,” *SAE Int. J. Fuels Lubr.*, vol. 6, no. 1, pp. 170–187, Apr. 2013, https://doi.org/10.4271/2013-01-1678.
[11] A. B. Dempsey, S. Curran, and R. D. Reitz, “Characterization of Reactivity Controlled Compression Ignition (RCCI) Using Premixed Gasoline and Direct-Injected Gasoline with a Cetane Improver on a Multi-Cylinder Engine,” *SAE Int. J. Engines*, vol. 8, no. 2, pp. 859–877, Apr. 2015, 10.4271/2015-01-0855.
[12] J. E. Dec and D. Lopez-Pintor, “Demonstrating the Potential of LTGC-AMFI to Deliver the Promise of Low-Temperature Combustion,” *Thermo and fluid dynamic processes in direct injection engines THIESEL*, Sep. 2020.
[13] D. Lopez Pintor, G. Gentz, and J. Dec, “Mixture Stratification for CA50 Control of LTGC Engines with Reactivity-Enhanced and Non-Additized Gasoline,” *SAE Technical Paper 2021-01-0513*, Apr. 2021, 10.4271/2021-01-0513.
[14] D. Lopez Pintor, J. E. Dec, and G. Gentz, “Experimental evaluation of a custom gasoline-like blend designed to simultaneously improve φ-sensitivity, RON and octane sensitivity,” *SAE Int. J. Adv. & Curr. Prac. in Mobility*, vol. 2, no. 4, pp. 2196–2216, 2020, https://doi.org/10.4271/2020-01-1136.
[15] H. O. Pritchard, “Thermal decomposition of isooctyl nitrate,” *Combustion and Flame*, vol. 75, no. 3, pp. 415–416, Mar. 1989, 10.1016/0010-2180(89)90052-7.
[16] Y. Stein, R. A. Yetter, F. L. Dryer, and A. Aradi, “The Autoignition Behavior of Surrogate Diesel Fuel Mixtures and the Chemical Effects of 2-Ethylhexyl Nitrate (2-EHN) Cetane Improver,” presented at the International Fuels & Lubricants Meeting & Exposition, 1999, pp. 1999-01–1504.
[17] M. Hartmann *et al.*, “Experiments and modeling of ignition delay times, flame structure and intermediate species of EHN-doped stoichiometric n-heptane/air combustion,” *Proceedings of the Combustion Institute*, vol. 32, no. 1, pp. 197–204, Jan. 2009, 10.1016/j.proci.2008.06.068.
[18] S. S. Goldsborough, M. V. Johnson, C. Banyon, W. J. Pitz, and M. J. McNenly, “Experimental and modeling study of fuel interactions with an alkyl nitrate cetane

enhancer, 2-ethyl-hexyl nitrate," *Proceedings of the Combustion Institute*, vol. 35, no. 1, pp. 571–579, Jan. 2015, 10.1016/j.proci.2014.06.048.
[19] J. C. G. Andrae, "Semidetailed Kinetic Model for Gasoline Surrogate Fuel Interactions with the Ignition Enhancer 2-Ethylhexyl Nitrate," *Energy Fuels*, vol. 29, no. 6, pp. 3944–3952, Jun. 2015, 10.1021/acs.energyfuels.5b00589.
[20] B. D. Adhikary, "Low load operation in a light-duty diesel engine using high octane fuels and additives," University of Wisconsin – Madison, 2014.
[21] D. Lopez Pintor and J. E. Dec, "Development and validation of an EHN mechanism for fundamental and applied chemistry studies," *SAE Technical Paper 2022-01-0455*, 2022, https://doi.org/10.4271/2022-01-0455.
[22] S. Cheng *et al.*, "Autoignition and preliminary heat release of gasoline surrogates and their blends with ethanol at engine-relevant conditions: Experiments and comprehensive kinetic modeling," *Combustion and Flame*, vol. 228, pp. 57–77, Jun. 2021, 10.1016/j.combustflame.2021.01.033.
[23] C. A. Almodovar and C. F. Goldsmith, "Laser schlieren study of the thermal decomposition of 2-ethylhexyl-nitrate," *Proceedings of the Combustion Institute*, vol. 38, no. 1, pp. 997–1005, Jan. 2021, 10.1016/j.proci.2020.07.105.
[24] J. C. Oxley, J. L. Smith, E. Rogers, W. Ye, A. A. Aradi, and T. J. Henly, "Fuel Combustion Additives: A Study of Their Thermal Stabilities and Decomposition Pathways," *Energy Fuels*, vol. 14, no. 6, pp. 1252–1264, Nov. 2000, 10.1021/ef000101i.
[25] S. N. Gadhvi, "Relationship between Fuel Properties and Cetane Response of Cetane Improver for Non-Aromatic and Aromatic Fuels Used In A Single Cylinder Heavy Duty Diesel Engine," *Petroleum and Chemical Industry International*, vol. 2, no. 1, pp. 1–5, 2019.
[26] S. Cheng, S. S. Goldsborough, S. W. Wagnon, and W. J. Pitz, "Probing intermediate temperature heat release in autoignition of C3-C4 iso-alcohol/gasoline blends," *Combustion and Flame*, vol. 233, p. 111602, Nov. 2021, 10.1016/j.combustflame.2021.111602.
[27] S. Cheng, S. Scott Goldsborough, C. Saggese, S. W. Wagnon, and W. J. Pitz, "New insights into fuel blending effects: Intermolecular chemical kinetic interactions affecting autoignition times and intermediate-temperature heat release," *Combustion and Flame*, vol. 233, p. 111559, Nov. 2021, 10.1016/j.combustflame.2021.111559.
[28] V. L. Dagle *et al.*, "Production, fuel properties and combustion testing of an iso-olefins blendstock for modern vehicles," *Fuel*, vol. 310, p. 122314, Feb. 2022, 10.1016/j.fuel.2021.122314.
[29] S. S. Goldsborough, S. Cheng, D. Kang, C. Saggese, S. W. Wagnon, and W. J. Pitz, "Effects of isoalcohol blending with gasoline on autoignition behavior in a rapid compression machine: Isopropanol and isobutanol," *Proceedings of the Combustion Institute*, vol. 38, no. 4, pp. 5655–5664, Jan. 2021, 10.1016/j.proci.2020.08.027.
[30] C. Michelbach and A. Tomlin, "An experimental and kinetic modeling study of the ignition delay and heat release characteristics of a five component gasoline surrogate and its blends with iso-butanol within a rapid compression machine," *International Journal of Chemical Kinetics*, vol. 53, no. 6, pp. 787–808, 2021, https://doi.org/10.1002/kin.21483.
[31] S. S. Goldsborough, S. Hochgreb, G. Vanhove, M. S. Wooldridge, H. J. Curran, and C.-J. Sung, "Advances in rapid compression machine studies of low- and intermediate-temperature autoignition phenomena," *Progress in Energy and Combustion Science*, vol. 63, pp. 1–78, Nov. 2017, 10.1016/j.pecs.2017.05.002.
[32] C. J. Sung and H. J. Curran, "Using rapid compression machines for chemical kinetics studies," *Progress in Energy and Combustion Science*, vol. 44, pp. 1–18, 2014.

[33] B. W. Weber and C.-J. Sung, “Comparative Autoignition Trends in Butanol Isomers at Elevated Pressure,” *Energy Fuels*, vol. 27, no. 3, pp. 1688–1698, Mar. 2013, 10.1021/ef302195c.
[34] T. Lu and C. K. Law, “A directed relation graph method for mechanism reduction,” *Proceedings of the Combustion Institute*, vol. 30, no. 1, pp. 1333–1341, Jan. 2005, 10.1016/j.proci.2004.08.145.
[35] P. Pepiot-Desjardins and H. Pitsch, “An efficient error-propagation-based reduction method for large chemical kinetic mechanisms,” *Combustion and Flame*, vol. 154, no. 1, pp. 67–81, Jul. 2008, 10.1016/j.combustflame.2007.10.020.
[36] K. E. Niemeyer, C. J. Sung, and M. P. Raju, “Skeletal mechanism generation for surrogate fuels using directed relation graph with error propagation and sensitivity analysis,” *Combustion and Flame*, vol. 157, pp. 1760–1770, 2010.
[37] A. M. Ickes, S. V. Bohac, and D. N. Assanis, “Effect of 2-Ethylhexyl Nitrate Cetane Improver on NOx Emissions from Premixed Low-Temperature Diesel Combustion,” *Energy Fuels*, vol. 23, no. 10, pp. 4943–4948, Oct. 2009, 10.1021/ef900408e.
[38] F. Contino, F. Foucher, P. Dagaut, T. Lucchini, G. D’Errico, and C. Mounaïm-Rousselle, “Experimental and numerical analysis of nitric oxide effect on the ignition of iso-octane in a single cylinder HCCI engine,” *Combustion and Flame*, vol. 160, no. 8, pp. 1476–1483, Aug. 2013, 10.1016/j.combustflame.2013.02.028.

Appendix A. Evaluation of the reduced PRF mechanism

Figures A1-4 show the ignition delay obtained in a 0D closed adiabatic constant-volume reactor with the detailed mechanism and with the reduced mechanism for PRF0, PRF40, PRF60 and PRF100, respectively. Simulations were performed at wide ranges of pressure and temperature for equivalence ratio 0.4 and 21% O_2. In general, the reduced mechanism shows a reasonably good agreement with the detailed mechanism; between mechanisms, the largest deviation of ignition delay is 71%, and the average of deviation is 10%.

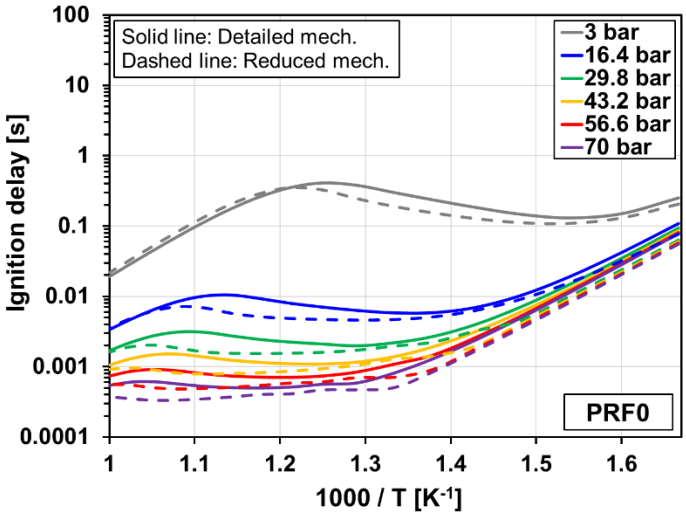

Figure A1. Ignition delay of PRF0 (n-heptane) for equivalence ratio 0.4 and 21% O_2 at several temperatures and pressures.

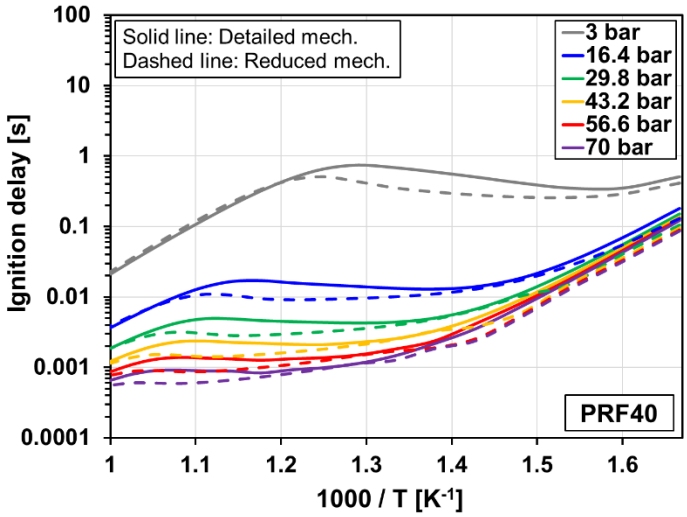

634

635 *Figure A2. Ignition delay of PRF40 (40%$_{vol}$ iso-octane + 60%$_{vol}$ n-heptane) for equivalence ratio 0.4 and*
636 *21% O_2 at several temperatures and pressures.*

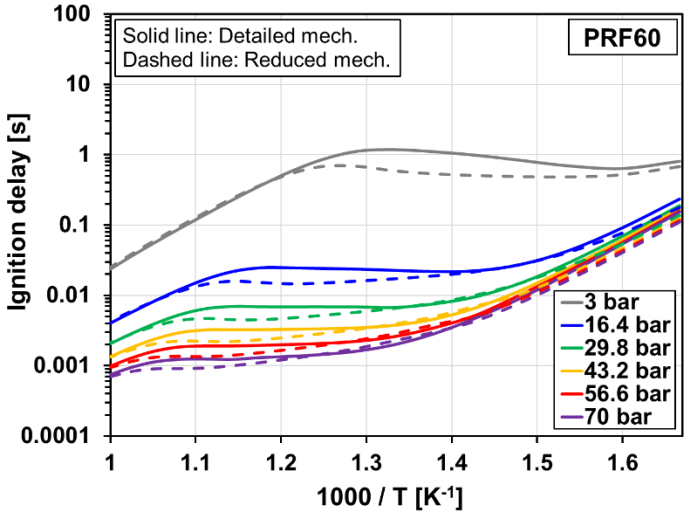

637

638 *Figure A3. Ignition delay of PRF60 (60%$_{vol}$ iso-octane + 40%$_{vol}$ n-heptane) for equivalence ratio 0.4 and*
639 *21% O_2 at several temperatures and pressures.*

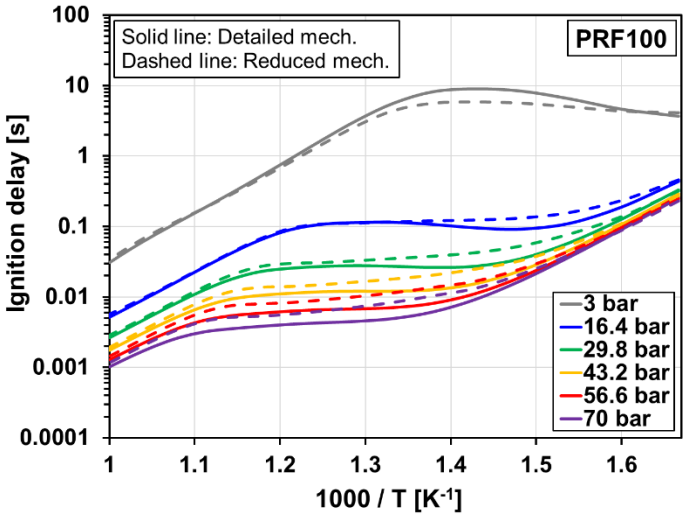

Figure A4. Ignition delay of PRF1000 (iso-octane) for equivalence ratio 0.4 and 21% O_2 at several temperatures and pressures.